Advances in Applied Mathematics and Mechanics
Adv. Appl. Math. Mech., Vol. 7, No. 6, pp. 715-735

DOI: 10.4208/aamm.2014.m464
December 2015

A Simplified Parallel Two-Level Iterative Method for Simulation of Incompressible Navier-Stokes Equations

Yueqiang Shang[1,*] and Jin Qin[2]

[1] *School of Mathematics and Statistics, Southwest University, Chongqing 400715, China*
[2] *School of Mathematics and Computer Science, Zunyi Normal College, Zunyi 563002, China*

Received 12 January 2014; Accepted (in revised version) 12 November 2014

Abstract. Based on two-grid discretization, a simplified parallel iterative finite element method for the simulation of incompressible Navier-Stokes equations is developed and analyzed. The method is based on a fixed point iteration for the equations on a coarse grid, where a Stokes problem is solved at each iteration. Then, on overlapped local fine grids, corrections are calculated in parallel by solving an Oseen problem in which the fixed convection is given by the coarse grid solution. Error bounds of the approximate solution are derived. Numerical results on examples of known analytical solutions, lid-driven cavity flow and backward-facing step flow are also given to demonstrate the effectiveness of the method.

AMS subject classifications: 65N55, 76D07, 76M10

Key words: Navier-Stokes equations, finite element, two-level method, parallel algorithm.

1 Introduction

With the development of technology for parallel computation, parallel computing attracts more and more attentions in computational fluid dynamics community nowadays. In such parallel computing, parallel algorithms play a key role in exploiting the full potential of the computational power of parallel computers and ensuring the accuracy of the approximate solution. Therefore, much effort is thrown to the development of efficient parallel numerical methods for the Navier-Stokes equations and related problems.

Recently, based on the two-grid discretization approach of Xu and Zhou [1, 2], and motivated by the observation that for a finite element solution to the Navier-Stokes equations, low frequency components can be approximated well by a relatively coarse grid

*Corresponding author.
Email: yueqiangshang@gmail.com (Y. Q. Shang), shuxuexiqinjin@sina.com (J. Qin)

and high frequency components can be computed on a fine grid, some local and parallel algorithms were proposed by He et al. [3], Ma et al. [4,5], and Shang et al. [6,7]. In these algorithms, the fully nonlinear Navier-Stokes equations are first solved on a coarse grid, and then corrections are calculated locally or in parallel by solving a linear problem on a fine grid. Numerical tests showed the efficiency of the algorithms [5–8]. Furthermore, by combing classical iterative methods for the Navier-Stokes equations with this approach to local and parallel finite element computations, some parallel iterative algorithms were developed and analyzed in [9,10]. This local and parallel finite element computation approach was also combined with the variational multiscale method [11] and the subgrid stabilization method [12].

In this paper, based on two-grid finite element discretization and using domain decomposition technique, we develop a simplified parallel iterative method for the simulation of incompressible flows governed by the Navier-Stokes equations. It uses a fixed point iteration that differs from those used in [9,10] for the nonlinear Navier-Stokes equations on a coarse grid, where Stokes problems are solved, and then solves an Oseen problem in a parallel manner on a fine grid to correct the solution, where the convection term is fixed by the coarse grid solution. Compared to the methods of [9,10] where Newton and Oseen iterations were employed, this method only solves a linear Stokes problem (hence, linear with positive definite symmetric part) at each iteration. Specifically, we first iteratively solve the Navier-Stokes problem by solving a sequence of Stokes equations on a coarse grid, and then compute fine grid corrections in a parallel manner by solving a linearized Oseen problem in overlapped subdomains. This method has low communication complexity. It only requires an existing sequential solver as subproblem solver and hence can reuse existing sequential software. Under the stability condition $\frac{4N}{\nu^2}\|f\|_{-1,\Omega}<1$ (here N is defined by (2.3), ν is the kinematic viscosity of the fluid, and f the external body force exerting on the fluid), we derive the following error estimate for our parallel method:

$$
\begin{aligned}
&|||\nabla(u-u_m^h)|||_{0,\Omega}+|||p-p_m^h|||_{0,\Omega}\\
\le& c\big(h^s+H^{s+1}(1+\|f\|_{0,\Omega})\big)\|f\|_{s-1,\Omega}+C\Big(\frac{3N}{\nu^2}\|f\|_{-1,\Omega}\Big)^m\|f\|_{-1,\Omega}, \quad 1\le s\le k, \quad m\ge 1,
\end{aligned}
\tag{1.1}
$$

where $|||\cdot|||_{0,\Omega}$ is piecewise norm defined by (3.3), m the number of nonlinear iterations satisfying the stopping criterion, (u,p) the exact solution to the Navier-Stokes equations, (u_m^h,p_m^h) the solution obtained from our parallel finite element method, H and h are the coarse and fine grids sizes, respectively, c and C are two generic positive constants which are independent of mesh parameter and may stand for different values at their different occurrences in our paper, k and s are two positive constants related to the regularity of the solution (u,p) to the Navier-Stokes equations and the finite element spaces used for the discretization, respectively; see Theorem 3.2.

The above estimate shows that if we choose the coarse grid size H such that $H=\mathcal{O}(h^{\frac{s}{s+1}})$, then a convergence rate of the same order as the standard Galerkin finite element method in H^1-norm for the velocity and L^2-norm for the pressure can be obtained by our parallel method. However, due to that only a linear problem needs to be solved in parallel on the fine grid, our method can save a large amount of computational time.

The paper is organized as follows. In the next section, the functional setting of the Navier-Stokes equations and some assumptions on mixed finite element spaces are provided. Based on two-grid discretization, parallel two-level finite element algorithms are developed and analyzed in Section 3. In Section 4, some numerical results are given to illustrate the effectiveness of the parallel method. Finally, concluding remarks complete the paper.

2 Preliminaries

As usual, for a nonnegative integer l, we denote by $H^l(\Omega)$ the Sobolev space of functions with square integrable distribution derivatives up to order l in Ω, equipped with the standard norm $\|\cdot\|_{l,\Omega}$; while denote by $H_0^1(\Omega)$ the closed subspace of $H^1(\Omega)$ consisting of functions with zero trace on $\partial\Omega$; see, e.g., [13]. The space $H^{-1}(\Omega)$, the dual space of $H_0^1(\Omega)$, and its associated norm $\|\cdot\|_{-1,\Omega}$ will also be used. Moreover, for a subdomain $\Omega_0\subset\Omega$, we view $H_0^1(\Omega_0)$ as a subspace of $H_0^1(\Omega)$ by extending the functions in $H_0^1(\Omega_0)$ to be functions in $H_0^1(\Omega)$ with zero outside of Ω_0. For a subdomain D, we use the notation $D\subset\subset\Omega_0$ to mean that $\mathrm{dist}(\partial D\backslash\partial\Omega,\partial\Omega_0\backslash\partial\Omega)>0$).

2.1 Functional setting of the Navier-Stokes equations

Let Ω be a bounded domain with Lipschitz-continuous boundary $\partial\Omega$ in $\mathbb{R}^d$ $(d=2,3)$. We consider the following incompressible Navier-Stokes equations:

$$-\nu\Delta u+(u\cdot\nabla)u+\nabla p=f \qquad \text{in } \Omega, \tag{2.1a}$$

$$\mathrm{div} u=0, \qquad \text{in } \Omega, \tag{2.1b}$$

$$u=0 \qquad \text{on } \partial\Omega, \tag{2.1c}$$

where $u=(u_1,\cdots,u_d)$ is the velocity, p the pressure, $f=(f_1,\cdots,f_d)$ the prescribed body force and ν the kinematic viscosity.

To introduce the variational formulation of problem (2.1a)-(2.1c), we set

$$X=H_0^1(\Omega)^d, \quad Y=L^2(\Omega)^d, \quad M=L_0^2(\Omega)=\Big\{q\in L^2(\Omega):\ \int_\Omega q dx=0\Big\},$$

and define $a(\cdot,\cdot)$, $b(\cdot,\cdot,\cdot)$, $d(\cdot,\cdot)$ as

$$\begin{aligned} &a(u,v)=\nu(\nabla u,\nabla v), \quad b(u,v,w)=\frac{1}{2}((u\cdot\nabla)v,w)-\frac{1}{2}((u\cdot\nabla)w,v),\\ &d(v,q)=(\mathrm{div}\ v,q), \quad \forall u,v,w\in X,\ q\in M, \end{aligned}$$

where $(\cdot,\cdot)$ is the standard inner-product of $L^2(\Omega)^\theta$ $(\theta=1,2,3)$.

It is well known that the trilinear term $b(\cdot,\cdot,\cdot)$ has the following properties (cf. [14,15]):

$$b(u,v,w)=-b(u,w,v), \qquad \forall u,v,w\in X, \tag{2.2a}$$
$$|b(u,v,w)|\le N\|\nabla u\|_{0,\Omega}\|\nabla v\|_{0,\Omega}\|\nabla w\|_{0,\Omega}, \qquad \forall u,v,w\in X, \tag{2.2b}$$

where

$$N=\sup_{\substack{u,v,w\in X,\\ u,v,w\neq 0}}\frac{|b(u,v,w)|}{\|\nabla u\|_{0,\Omega}\|\nabla v\|_{0,\Omega}\|\nabla w\|_{0,\Omega}}. \tag{2.3}$$

With the above notations, the variational formulation of (2.1a)-(2.1c) reads: find a pair $(u,p)\in X\times M$ such that

$$a(u,v)+b(u,u,v)-d(v,p)+d(u,q)=(f,v), \quad \forall (v,q)\in X\times M. \tag{2.4}$$

We have the following existence and uniqueness results (cf. [15,16]).

Theorem 2.1. *Let Ω be a C^{k+1}-smooth bounded domain in $\mathbb{R}^d$ for $k\ge 1$ or a bounded convex polygonal or polyhedral domain in $\mathbb{R}^d$ for $k=1$. Given $f\in H^{k-1}(\Omega)^d$, problem* (2.4) *admits at least a solution pair $(u,p)\in (H^{k+1}(\Omega)\cap H_0^1(\Omega))^d\times (H^k(\Omega)\cap L_0^2(\Omega))$ satisfying*

$$\|\nabla u\|_{0,\Omega}\le \nu^{-1}\|f\|_{-1,\Omega}, \quad \|f\|_{-1,\Omega}=\sup_{\substack{v\in X,\\ v\neq 0}}\frac{|(f,v)|}{\|\nabla v\|_{0,\Omega}}, \tag{2.5a}$$
$$\nu\|u\|_{s+1,\Omega}+\|p\|_{s,\Omega}\le c\|f\|_{s-1,\Omega}, \quad 0\le s\le k. \tag{2.5b}$$

Moreover, if ν and f satisfy the following uniqueness condition:

$$\frac{N\|f\|_{-1,\Omega}}{\nu^2}<1, \tag{2.6}$$

then the solution pair (u,p) of problem (2.4) *is unique.*

2.2 Finite element spaces

Assume that $T^h(\Omega)=\{K\}$ is a mesh of Ω with a mesh-size function $h(x)$ whose value is the diameter h_K of the element K containing x. One basic assumption on the mesh is that it is not exceedingly over-refined locally, namely [1,3],

A0. Triangulation. There exists $\gamma\ge 1$ such that

$$h_\Omega^\gamma\le ch(x), \quad \forall x\in\Omega, \tag{2.7}$$

where $h_\Omega=\max_{x\in\Omega}h(x)$ is the largest mesh size of $T^h(\Omega)$. Sometimes, we shall drop the subscript in h_Ω and use h for the mesh size on a domain that is clear from the context.

Associated with a mesh $T^h(\Omega)$, let $X_h(\Omega)\subset H^1(\Omega)^d$, $M_h(\Omega)\subset L^2(\Omega)$ be two finite element spaces and

$$X_h^0(\Omega)=X_h(\Omega)\cap H_0^1(\Omega)^d,\quad M_h^0(\Omega)=M_h(\Omega)\cap L_0^2(\Omega).$$

Given $G\subset\Omega$, we define $X_h(G)$, $M_h(G)$, and $T^h(G)$ to be the restriction of $X_h(\Omega)$, $M_h(\Omega)$ and $T^h(\Omega)$ to G, respectively, and set

$$X_0^h(G)=\{v\in X_h(\Omega):\text{supp } v\subset\subset G\},\quad M_0^h(G)=\{q\in M_h(\Omega):\text{supp } q\subset\subset G\}.$$

Some basic assumptions on the mixed finite element spaces are needed (cf. [3,5,17,18]).
A1. Approximation. For each $(u,p)\in H^{k+1}(G)^d\times H^k(G)$ $(k\geq 1)$, there exists an approximation $(\pi_h u,\rho_h p)\in X_h(G)\times M_h(G)$ such that

$$\|(u-\pi_h u)\|_{0,G}+\|h(u-\pi_h u)\|_{1,G}\leq ch_G^{s+1}\|u\|_{1+s,G},\qquad 1\leq s\leq k, \tag{2.8a}$$
$$\|(p-\rho_h p)\|_{-1,G}+\|h(p-\rho_h p)\|_{0,G}\leq ch_G^{s+1}\|p\|_{s,G},\qquad 1\leq s\leq k. \tag{2.8b}$$

A2. Inverse estimate. For any $(v,q)\in X_h(G)\times M_h(G)$, there hold

$$\|\nabla v\|_{0,G}\leq c\|h^{-1}v\|_{0,G},\quad \|q\|_{0,G}\leq c\|h^{-1}q\|_{-1,G}. \tag{2.9}$$

A3. Superapproximation. For $G\subset\Omega$, let $\omega\in C_0^\infty(\Omega)$ with supp $\omega\subset\subset G$. Then for any $(u,p)\in X_h(G)\times M_h(G)$, there is $(v,q)\in X_0^h(G)\times M_0^h(G)$ such that

$$\|h^{-1}\nabla(\omega u-v)\|_{0,G}\leq c\|\nabla u\|_{0,G},\quad \|h^{-1}(\omega p-q)\|_{0,G}\leq c\|p\|_{0,G}. \tag{2.10}$$

A4. Inf-sup condition. There exists a constant $\beta>0$ such that

$$\beta\|q\|_{0,G}\leq \sup_{\substack{v\in X_h^0(G),\\ v\neq 0}}\frac{(\text{div}v,q)}{\|\nabla v\|_{0,G}},\quad \forall q\in M_h^0(G). \tag{2.11}$$

We refer to [19] for some examples satisfying Assumptions A1-A4. For instance, the MINI finite elements [20] and the P_2-P_0 finite elements [21] satisfy Assumptions A1-A4 when $k=1$, while the Taylor-Hood elements [22] and the augmented P_2-P_1 elements [23, 24] satisfy Assumptions A1-A4 when $k=2$. Throughout this paper, we assume that $h\ll 1$ and Assumptions A0-A4 hold.

Under the above assumptions, the mixed finite element approximation of problem (2.4) reads: find a pair $(u_h,p_h)\in X_h^0(\Omega)\times M_h^0(\Omega)$ such that

$$a(u_h,v)+b(u_h,u_h,v)-d(v,p_h)+d(u_h,q)=(f,v),\quad \forall (v,q)\in X_h^0(\Omega)\times M_h^0(\Omega). \tag{2.12}$$

The following results on (u_h,p_h) are classical (cf. [3,15,16,25]).

Theorem 2.2. *Suppose that Assumptions A0, A1, A4 and the conditions of Theorem 2.1 hold. There exists a small* $h_0>0$ *such that for all* $h\in(0,h_0]$*, problem* (2.12) *admits a unique solution* (u_h,p_h) *satisfying*

$$\|\nabla u_h\|_{0,\Omega}\leq \nu^{-1}\|f\|_{-1,\Omega},\quad \|p_h\|_0\leq 3\beta^{-1}\|f\|_{-1,\Omega}, \tag{2.13a}$$

$$\nu\|\nabla(u-u_h)\|_{0,\Omega}+\|p-p_h\|_{0,\Omega}\leq ch^s\|f\|_{s-1,\Omega},\quad 1\leq s\leq k, \tag{2.13b}$$

$$\nu\|u-u_h\|_{0,\Omega}+\|p-p_h\|_{-1,\Omega}\leq ch^{s+1}\|f\|_{s-1,\Omega},\quad 1\leq s\leq k. \tag{2.13c}$$

3 Parallel finite element algorithms

In this section, based on two-grid discretization and overlapping domain decomposition, we shall firstly introduce a parallel finite element algorithm for problem (2.12), and the develop and analyze a two-level parallel iterative finite element algorithm.

3.1 Parallel finite element algorithm

Let $T^H(\Omega)$ be a shape-regular coarse grid with size $H\gg h$. We first divide Ω into a number of disjoint subdomains $D_1,\cdots,D_J$, and then enlarge each D_j to obtain Ω_j that align with $T^H(\Omega)$ and satisfy $D_j\subset\subset\Omega_j\subset\Omega$. These $\Omega_j's$ compose an overlapping decomposition of Ω. Assume $T^h(\Omega_j)$ to be a fine grid of subdomain Ω_j with size h which can be obtained from the mesh $T^H(\Omega)$. In our analysis, we shall use an auxiliary fine grid, say $T^h(\Omega)$, that is globally defined and coincides with $T^h(\Omega_j)$ on Ω_j; see Fig. 1.

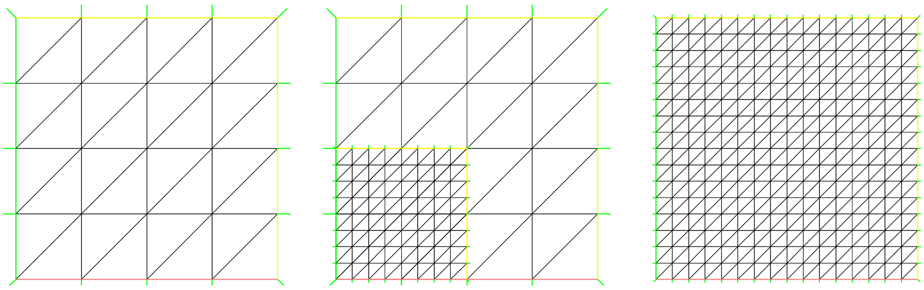

(a) (b) (c)

Figure 1: Meshes: (a) a global coarse mesh; (b) a local fine mesh; and (c) a global fine mesh.

Algorithm 3.1. Parallel finite element algorithm.

1. Find a global coarse grid solution $(u_H,p_H)\in X_H^0(\Omega)\times M_H^0(\Omega)$ such that

$$a(u_H,v)+b(u_H,u_H,v)-d(v,p_H)+d(u_H,q)=(f,v),\quad \forall(v,q)\in X_H^0(\Omega)\times M_H^0(\Omega). \tag{3.1}$$

2. Find local fine grid corrections $(e_{jh},\eta_{jh})\in X_h^0(\Omega_j)\times M_h^0(\Omega_j)$ $(j=1,2,\cdots,J)$ in parallel by solving the following Oseen equations:

$$\begin{aligned} &a(e_{jh},v)+b(u_H,e_{jh},v)-d(v,\eta_{jh})+d(e_{jh},q)\\ =&(f,v)-a(u_H,v)-b(u_H,u_H,v)+d(v,p_H)-d(u_H,q), \quad \forall (v,q)\in X_h^0(\Omega_j)\times M_h^0(\Omega_j). \end{aligned} \tag{3.2}$$

3. Set $(u^h,p^h)=(u_H,p_H)+(e_{jh},\eta_{jh})$ in D_j $(j=1,2,\cdots,J)$.

Defining piecewise norm

$$|||\cdot|||_{0,\Omega}=\Big(\sum_{j=1}^J\|\cdot\|^2_{0,D_j}\Big)^{1/2}, \tag{3.3}$$

we have the following results (cf. [3,10]).

Theorem 3.1. *Suppose that the conditions of Theorem 2.1 and Assumptions A0-A4 hold, $(u_h,p_h)\in X_h^0(\Omega)\times M_h^0(\Omega)$ is the standard Galerkin finite element solution of problem* (2.12), *(u^h,p^h) is obtained from Algorithm 3.1. Then*

$$|||\nabla(u_h-u^h)|||_{0,\Omega}+|||p_h-p^h|||_{0,\Omega}\le cH^{s+1}(1+\|f\|_{0,\Omega})\|f\|_{s-1,\Omega}, \quad 1\le s\le k. \tag{3.4}$$

Consequently,

$$|||\nabla(u-u^h)|||_{0,\Omega}+|||p-p^h|||_{0,\Omega}\le c\big(h^s+H^{s+1}(1+\|f\|_{0,\Omega})\big)\|f\|_{s-1,\Omega}, \quad 1\le s\le k. \tag{3.5}$$

Remark 3.1. From the definition of piecewise norm $|||\cdot|||_{0,\Omega}$ (see (3.3)), we can see that the constant c in (3.4) and (3.5) is relevant to the number J of subdomains, allowing the algorithm to be suitable for those parallel architectures with a moderate number of processors.

3.2 Simplified parallel two-level iterative finite element algorithm

We now discuss how to solve the nonlinear problem on the coarse grid in Algorithm 3.1. By applying a simple iteration of m times to the nonlinear problem, we can easily develop a parallel two-level iterative finite element algorithm for the Navier-Stokes equations.

Algorithm 3.2. Simplified parallel two-level iterative finite element algorithm.

1. Find a global coarse grid iterative solution $(u_H^m,p_H^m)\in X_H^0(\Omega)\times M_H^0(\Omega)$ such that

$$a(u_H^n,v)-d(v,p_H^n)+d(u_H^n,q)=(f,v)-b(u_H^{n-1},u_H^{n-1},v), \quad \forall (v,q)\in X_H^0(\Omega)\times M_H^0(\Omega), \tag{3.6}$$

for $n=1,\cdots,m$, with $u_H^0=0$.

2. Find local fine grid corrections $(e_{jh}^m,\eta_{jh}^m)\in X_h^0(\Omega_j)\times M_h^0(\Omega_j)$ $(j=1,2,\cdots,J)$ in parallel by solving the following Oseen equations:

$$\begin{aligned} &a(e_{jh}^m,v)+b(u_H^m,e_{jh}^m,v)-d(v,\eta_{jh}^m)+d(e_{jh}^m,q)\\ =&(f,v)-a(u_H^m,v)-b(u_H^m,u_H^m,v)+d(v,p_H^m)-d(u_H^m,q), \quad \forall (v,q)\in X_h^0(\Omega_j)\times M_h^0(\Omega_j). \end{aligned} \tag{3.7}$$

3. Set $(u_m^h,p_m^h)=(u_H^m,p_H^m)+(e_{jh}^m,\eta_{jh}^m)$ in D_j $(j=1,2,\cdots,J)$.

For the iterative scheme (3.6), we have the following results [26].

Lemma 3.1. *Under the following stability condition:*

$$\frac{4N}{\nu^2}\|f\|_{-1,\Omega}<1, \tag{3.8}$$

the sequence (u_H^n,p_H^n) defined by iterative scheme (3.6) *satisfies for all $n\geq 1$:*

$$\|\nabla u_H^n\|_{0,\Omega}\leq 2\nu^{-1}\|f\|_{-1,\Omega}, \quad \|p_H^n\|_{0,\Omega}\leq 4\beta^{-1}\|f\|_{-1,\Omega}, \tag{3.9a}$$

$$\nu\|\nabla(u_H-u_H^n)\|_{0,\Omega}+\|p_H-p_H^n\|_{0,\Omega}\leq c\Big(\frac{3N}{\nu^2}\|f\|_{-1,\Omega}\Big)^n\|f\|_{-1,\Omega}, \tag{3.9b}$$

$$\nu\|\nabla(u_H-u_H^n)\|_{0,\Omega}+\|p_H-p_H^n\|_{0,\Omega}\leq c\nu\|u_H^n-u_H^{n-1}\|_{0,\Omega}, \tag{3.9c}$$

where (u_H,p_H) is the standard finite element solution to the Navier-Stokes equations (2.4) *computed on a mesh with size H.*

For the first inequality of (3.9a), inequalities (3.9b) and (3.9c), we refer the readers to Lemma 4.1, Lemma 5.1 and Theorem 5.4 of [26], respectively. While for the second inequality of (3.9a), taking $q=0$ in (3.6), we get

$$\begin{aligned} d(v,p_H^n)&=a(u_H^n,v)-(f,v)+b(u_H^{n-1},u_H^{n-1},v)\\ &\leq\big(\nu\|\nabla u_H^n\|_{0,\Omega}+\|f\|_{-1,\Omega}+N\|\nabla u_H^{n-1}\|_{0,\Omega}^2\big)\|\nabla v\|_{0,\Omega}\\ &\leq\big(2\|f\|_{-1,\Omega}+\|f\|_{-1,\Omega}+\|f\|_{-1,\Omega}\big)\|\nabla v\|_{0,\Omega}, \end{aligned}$$

which, together with the *inf-sup* condition, follows the required result.

Remark 3.2. Our algorithm needs the stability condition (3.8), which can be verified in practice by estimating N and $\|f\|_{-1,\Omega}$. We refer to [27] for a discuss for this.

Remark 3.3. Estimate (3.9c) shows that $\|\nabla(u_H-u_H^n)\|_{0,\Omega}$ and $\|p_H-p_H^n\|_{0,\Omega}$ can be bounded by $\|u_H^n-u_H^{n-1}\|_{0,\Omega}$. This is true since (u_H,p_H), the solution of nonlinear finite element problem (3.1), is approximated by (u_H^n,p_H^n), the nth iterative solution of the finite element problem (3.6). The approximation depends on the simple nonlinear iterations. Given the convergence of the simple nonlinear iterations, $\|u_H^n-u_H^{n-1}\|_{0,\Omega}$ will tend to zero as n tends to infinity, which means that $C\|u_H^n-u_H^{n-1}\|_{0,\Omega}$ tends to zero as well even there is a constant C, and so (u_H^n,p_H^n) tends to (u_H,p_H). As for the problem that how accurate should the approximation be, we refer to the followed Remark 3.4.

Lemma 3.2. *Suppose that the conditions of Theorem 2.2 and Assumptions A0-A4 hold. Then e_{jh}^m $(j=1,2,\cdots,J)$ obtained from Algorithm 3.2 satisfies*

$$\nu\|\nabla e_{jh}^m\|_{0,\Omega_j}\leq c\|f\|_{-1,\Omega}, \tag{3.10}$$

where c is independent of ν.

Proof. Noting that Ω_j $(j=1,2,\cdots,J)$ align with $T^H(\Omega)$, (2.2b) also holds for Ω replaced by Ω_j. Taking $q=0$ in (3.7) and using the *inf-sup* condition (2.11), we get

$$\begin{aligned}\|\eta_{jh}^m\|_{0,\Omega_j} \le \beta^{-1}\big(&\nu\|\nabla e_{jh}^m\|_{0,\Omega_j} + N\|\nabla u_H^m\|_{0,\Omega_j}\|\nabla e_{jh}^m\|_{0,\Omega_j}\\ &+\|f\|_{-1,\Omega_j} + \nu\|\nabla u_H^m\|_{0,\Omega_j} + N\|\nabla u_H^m\|_{0,\Omega_j}^2 + c\|p_H^m\|_{0,\Omega_j}\big).\end{aligned} \tag{3.11}$$

Setting $(v,q)=(e_{jh}^m,\eta_{jh}^m)$ in (3.7), applying Young inequality, (2.2a) and (3.11), we arrive at

$$\begin{aligned}\nu\|\nabla e_{jh}^m\|_{0,\Omega_j}^2 \le& \|f\|_{-1,\Omega_j}\|\nabla e_{jh}^m\|_{0,\Omega_j} + \nu\|\nabla u_H^m\|_{0,\Omega_j}\|\nabla e_{jh}^m\|_{0,\Omega_j} + N\|\nabla u_H^m\|_{0,\Omega_j}^2\|\nabla e_{jh}^m\|_{0,\Omega_j}\\ &+c\|p_H^m\|_{0,\Omega_j}\|\nabla e_{jh}^m\|_{0,\Omega_j} + c\|\nabla u_H^m\|_{0,\Omega_j}\|\eta_{jh}^m\|_{0,\Omega_j}\\ \le& \frac{\nu}{8}\|\nabla e_{jh}^m\|_{0,\Omega_j}^2 + \frac{2}{\nu}\|f\|_{-1,\Omega_j}^2 + \frac{\nu}{8}\|\nabla e_{jh}^m\|_{0,\Omega_j}^2 + 2\nu\|\nabla u_H^m\|_{0,\Omega_j}^2\\ &+\frac{\nu}{8}\|\nabla e_{jh}^m\|_{0,\Omega_j}^2 + \frac{2N^2}{\nu}\|\nabla u_H^m\|_{0,\Omega_j}^4 + \frac{\nu}{8}\|\nabla e_{jh}^m\|_{0,\Omega_j}^2 + \frac{c}{\nu}\|p_H^m\|_{0,\Omega_j}^2\\ &+\frac{\nu}{8}\|\nabla e_{jh}^m\|_{0,\Omega_j}^2 + \frac{c\nu}{\beta^2}\|\nabla u_H^m\|_{0,\Omega_j}^2 + \frac{\nu}{8}\|\nabla e_{jh}^m\|_{0,\Omega_j}^2 + \frac{cN^2}{\beta^2\nu}\|\nabla u_H^m\|_{0,\Omega_j}^4\\ &+\frac{1}{2\nu}\|f\|_{-1,\Omega_j}^2 + \frac{c\nu}{2\beta^2}\|\nabla u_H^m\|_{0,\Omega_j}^2 + \frac{c\nu}{\beta}\|\nabla u_H^m\|_{0,\Omega_j}^2 + \frac{cN}{\beta}\|\nabla u_H^m\|_{0,\Omega_j}^3\\ &+\frac{c\nu}{4\beta^2}\|\nabla u_H^m\|_{0,\Omega_j}^2 + \frac{c}{\nu}\|p_H^m\|_{0,\Omega_j}^2.\end{aligned}$$

Thus

$$\nu\|\nabla e_{jh}^m\|_{0,\Omega_j}^2 \le c\Big(\frac{1}{\nu}\|f\|_{-1,\Omega_j}^2 + \nu\|\nabla u_H^m\|_{0,\Omega_j}^2 + \frac{N^2}{\nu}\|\nabla u_H^m\|_{0,\Omega_j}^4 + N\|\nabla u_H^m\|_{0,\Omega_j}^3 + \frac{1}{\nu}\|p_H^m\|_{0,\Omega_j}^2\Big).$$

Consequently, from (3.9a) and the stability condition (3.8), we obtain

$$\begin{aligned}\nu\|\nabla e_{jh}^m\|_{0,\Omega_j} \le& c\Big(\|f\|_{-1,\Omega_j} + \nu\|\nabla u_H^m\|_{0,\Omega_j} + N\|\nabla u_H^m\|_{0,\Omega_j}^2 + \sqrt{N\nu}\|\nabla u_H^m\|_{0,\Omega_j}^{3/2} + \|p_H^m\|_{0,\Omega_j}\Big)\\ \le& c\Big(3\|f\|_{-1,\Omega} + \frac{4N}{\nu^2}\|f\|_{-1,\Omega}^2 + \frac{2\sqrt{2N}}{\nu}\|f\|_{-1,\Omega}^{3/2} + \frac{4}{\beta}\|f\|_{-1,\Omega}\Big)\\ \le& c\|f\|_{-1,\Omega},\end{aligned}$$

which completes the proof. □

Lemma 3.3. *Assume that Assumptions A0-A4 and Theorem 2.2 hold,* (u^h,p^h) *and* (u_m^h,p_m^h) *are obtained from Algorithm 3.1 and Algorithm 3.2, respectively. Then under the stability condition* (3.8)*, we have, for* $j=1,2,\cdots,J$*, that*

$$\nu\|\nabla(u^h-u_m^h)\|_{0,D_j} + \|p^h-p_m^h\|_{0,D_j} \le c(\nu\|\nabla(u_H-u_H^m)\|_{0,\Omega_j} + \|p_H-p_H^m\|_{0,\Omega_j}),$$

where (u_H,p_H) *and* (u_H^m,p_H^m) *are the coarse grid solutions defined by Algorithm 3.1 and Algorithm 3.2, respectively.*

Proof. From Algorithm 3.1 and Algorithm 3.2, we get

$$
\begin{aligned}
&a(u_H+e_{jh},v)+b(u_H,e_{jh}+u_H,v)-d(v,p_H+\eta_{jh})+d(u_H+e_{jh},q)\\
&=(f,v), \qquad \forall(v,q)\in X_h^0(\Omega_j)\times M_h^0(\Omega_j), &(3.12a)\\
&a(u_H^m+e_{jh}^m,v)+b(u_H^m,e_{jh}^m+u_H^m,v)-d(v,p_H^m+\eta_{jh}^m)+d(u_H^m+e_{jh}^m,q)\\
&=(f,v), \qquad \forall(v,q)\in X_h^0(\Omega_j)\times M_h^0(\Omega_j). &(3.12b)
\end{aligned}
$$

Setting $(w_j,r_j)=(e_{jh}-e_{jh}^m,\eta_{jh}-\eta_{jh}^m)$, we see from (3.12a)-(3.12b) that

$$
\begin{aligned}
&a(u_H-u_H^m+w_j,v)+b(u_H,u_H-u_H^m+w_j,v)-d(v,r_j)+d(u_H-u_H^m+w_j,q)\\
=&(g,v), \quad \forall(v,q)\in X_h^0(\Omega_j)\times M_h^0(\Omega_j),
\end{aligned}
\tag{3.13}
$$

where

$$
(g,v)=d(v,p_H-p_H^m)-b(u_H-u_H^m,e_{jh}^m+u_H^m,v). \tag{3.14}
$$

By applying (2.2b), Theorem 2.2, Lemmas 3.1 and 3.2 and the stability condition (3.8), we obtain

$$
\begin{aligned}
\|g\|_{-1,\Omega_j}\le& c\|p_H-p_H^m\|_{0,\Omega_j}+N(\|\nabla u_H^m\|_{0,\Omega_j}+\|\nabla e_{jh}^m\|_{0,\Omega_j})\|\nabla(u_H-u_H^m)\|_{0,\Omega_j}\\
\le& c\|p_H-p_H^m\|_{0,\Omega_j}+c\frac{N}{\nu}\|f\|_{-1,\Omega}\cdot\|\nabla(u_H-u_H^m)\|_{0,\Omega_j}\\
\le& C\big(\|p_H-p_H^m\|_{0,\Omega_j}+\nu\|\nabla(u_H-u_H^m)\|_{0,\Omega_j}\big).
\end{aligned}
\tag{3.15}
$$

Therefore, taking $q=0$ in (3.13) and from the *inf-sup* condition (2.11), (2.13a) and (2.6), we get

$$
\begin{aligned}
\|r_j\|_{0,\Omega_j}\le&\beta^{-1}(\nu\|\nabla(u_H-u_H^m)\|_{0,\Omega_j}+\nu\|\nabla w_j\|_{0,\Omega_j}+\|g\|_{-1,\Omega_j})\\
&+\frac{N}{\beta}\|\nabla u_H\|_{0,\Omega_j}(\|\nabla(u_H-u_H^m)\|_{0,\Omega_j}+\|\nabla w_j\|_{0,\Omega_j})\\
\le& c\big(\nu\|\nabla(u_H-u_H^m)\|_{0,\Omega_j}+\nu\|\nabla w_j\|_{0,\Omega_j}+\|p_H-p_H^m\|_{0,\Omega_j}\big).
\end{aligned}
\tag{3.16}
$$

Taking $(v,q)=(w_j,r_j)$ in (3.13), using (2.2a) and the identity $2(a,a-b)=a^2-b^2+(a-b)^2$ with $a=\nabla(u^h-u_m^h)=\nabla(u_H-u_H^m+w_j)$ and $b=\nabla(u_H-u_H^m)$ for the first term in (3.13), we arrive at

$$
\begin{aligned}
&\frac{\nu}{2}\|\nabla(u^h-u_m^h)\|_{0,D_j}^2+\frac{\nu}{2}\|\nabla w_j\|_{0,\Omega_j}^2+b(u_H,u_H-u_H^m,w_j)\\
\le&\frac{\nu}{2}\|\nabla(u_H-u_H^m)\|_{0,\Omega_j}^2-d(u_H-u_H^m,r_j)+(g,w_j).
\end{aligned}
\tag{3.17}
$$

From (2.2b), (2.6), (2.13a), the stability condition (3.8), Young inequality and (3.16), we see

$$\begin{aligned}|b(u_H,u_H-u_H^m,w_j)| &\le N\|\nabla u_H\|_{0,\Omega_j}\|\nabla(u_H-u_H^m)\|_{0,\Omega_j}\|\nabla w_j\|_{0,\Omega_j}\\ &\le \frac{N}{\nu}\|f\|_{-1,\Omega}\|\nabla(u_H-u_H^m)\|_{0,\Omega_j}\|\nabla w_j\|_{0,\Omega_j}\\ &\le \frac{\nu}{8}\|\nabla w_j\|^2_{0,\Omega_j}+\frac{\nu}{8}\|\nabla(u_H-u_H^m)\|^2_{0,\Omega_j},\\ |d(u_H-u_H^m,r_j)| &\le c\|\nabla(u_H-u_H^m)\|_{0,\Omega_j}\|r_j\|_{0,\Omega_j}\\ &\le c\big(\nu\|\nabla(u_H-u_H^m)\|^2_{0,\Omega_j}+\nu\|\nabla(u_H-u_H^m)\|_{0,\Omega_j}\|\nabla w_j\|_{0,\Omega_j}\big)\\ &\quad +c\|\nabla(u_H-u_H^m)\|_{0,\Omega_j}\|p_H-p_H^m\|_{0,\Omega_j}\\ &\le \frac{\nu}{8}\|\nabla w_j\|^2_{0,\Omega_j}+c(\nu\|\nabla(u_H-u_H^m)\|^2_{0,\Omega_j}+\nu^{-1}\|p_H-p_H^m\|^2_{0,\Omega_j}),\\ |(g,w_j)| &\le \frac{\nu}{8}\|\nabla w_j\|^2_{0,\Omega_j}+2\nu^{-1}\|g\|^2_{-1,\Omega_j}.\end{aligned}$$

Taking the above inequalities into (3.17) and using (3.15), we deduce

$$\nu\|\nabla(u^h-u_m^h)\|_{0,D_j}+\nu\|\nabla w_j\|_{0,\Omega_j}\le c(\nu\|\nabla(u_H-u_H^m)\|_{0,\Omega_j}+\|p_H-p_H^m\|_{0,\Omega_j}). \tag{3.18}$$

Thus, the triangle inequality, (3.16) and (3.18) yield

$$\|p^h-p_m^h\|_{0,D_j}\le\|p_H-p_H^m\|_{0,D_j}+\|r_j\|_{0,D_j}\le c(\nu\|\nabla(u_H-u_H^m)\|_{0,\Omega_j}+\|p_H-p_H^m\|_{0,\Omega_j}). \tag{3.19}$$

Combining (3.18) with (3.19), we complete the proof. □

Theorem 3.2. *Suppose that Assumptions A0-A4 hold, (u_h,p_h) is the standard Galerkin finite element solution to the Navier-Stokes equations, (u_m^h,p_m^h) is obtained from Algorithm 3.2. Then under the conditions of Theorem 2.2 and the stability condition* (3.8), *the following error estimates hold:*

$$\begin{aligned}&|||\nabla(u_h-u_m^h)|||_{0,\Omega}+|||p_h-p_m^h|||_{0,\Omega}\\ &\le cH^{s+1}(1+\|f\|_{0,\Omega})\|f\|_{s-1,\Omega}+C\Big(\frac{3N}{\nu^2}\|f\|_{-1,\Omega}\Big)^m\|f\|_{-1,\Omega},\quad 1\le s\le k,\quad m\ge1,\end{aligned} \tag{3.20a}$$

$$\begin{aligned}&|||\nabla(u_h-u_m^h)|||_{0,\Omega}+|||p_h-p_m^h|||_{0,\Omega}\\ &\le cH^{s+1}(1+\|f\|_{0,\Omega})\|f\|_{s-1,\Omega}+C\|u_H^m-u_H^{m-1}\|_{0,\Omega},\quad 1\le s\le k,\quad m\ge1.\end{aligned} \tag{3.20b}$$

Consequently,

$$\begin{aligned}&|||\nabla(u-u_m^h)|||_{0,\Omega}+|||p-p_m^h|||_{0,\Omega}\\ &\le c\big(h^s+H^{s+1}(1+\|f\|_{0,\Omega})\big)\|f\|_{s-1,\Omega}\\ &\quad+C\Big(\frac{3N}{\nu^2}\|f\|_{-1,\Omega}\Big)^m\|f\|_{-1,\Omega},\quad 1\le s\le k,\quad m\ge1,\end{aligned} \tag{3.21a}$$

$$\begin{aligned}&|||\nabla(u-u_m^h)|||_{0,\Omega}+|||p-p_m^h|||_{0,\Omega}\\ &\le c\big(h^s+H^{s+1}(1+\|f\|_{0,\Omega})\big)\|f\|_{s-1,\Omega}+C\|u_H^m-u_H^{m-1}\|_{0,\Omega},\quad 1\le s\le k,\quad m\ge1.\end{aligned} \tag{3.21b}$$

Proof. By applying the triangle inequality, Lemmas 3.1 and 3.3, Theorem 3.1, we get

$$
\begin{aligned}
&|||\nabla(u_h-u_m^h)|||_{0,\Omega}+|||p_h-p_m^h|||_{0,\Omega}\\
&\le|||\nabla(u_h-u^h)|||_{0,\Omega}+|||\nabla(u^h-u_m^h)|||_{0,\Omega}+|||p_h-p^h|||_{0,\Omega}+|||p^h-p_m^h|||_{0,\Omega}\\
&\le cH^{s+1}(1+\|f\|_{0,\Omega})\|f\|_{s-1,\Omega}+C\Big(\frac{3N}{\nu^2}\|f\|_{-1,\Omega}\Big)^m\|f\|_{-1,\Omega},\quad 1\le s\le k,\quad m\ge 1,\\
&|||\nabla(u_h-u_m^h)|||_{0,\Omega}+|||p_h-p_m^h|||_{0,\Omega}\\
&\le cH^{s+1}(1+\|f\|_{0,\Omega})\|f\|_{s-1,\Omega}+C\|u_H^m-u_H^{m-1}\|_{0,\Omega},\quad 1\le s\le k,\quad m\ge 1,
\end{aligned}
$$

where (u^h,p^h) is the solution defined by Algorithm 3.1. Combining the triangle inequality with (2.13b) and (3.20a)-(3.20b), we get (3.21a)-(3.21b) and finish the proof. □

Remark 3.4. Theorem 3.2 shows that the error of the approximate solution consists of two parts: one is the discretization error depending on the underlying meshes, and the other is the error related to the simple nonlinear iterations on the coarse grid. If we choose the coarse grid size H such that $H=\mathcal{O}(h^{\frac{s}{s+1}})$, and solve the coarse grid problem to the accuracy satisfying $\|_H^m-u_H^{m-1}\|_{0,\Omega}=\mathcal{O}(h^s)$, then an optimal convergence rate can be obtained, and this indicates a stopping criterion for the simple nonlinear iterations on the coarse grid:

$$
\|u_H^m-u_H^{m-1}\|_{0,\Omega}<ch^s. \tag{3.22}
$$

4 Numerical results

In this section, we shall present some numerical results to illustrate the effectiveness of our parallel finite element method. Four numerical tests are performed: the first two test cases are 2D and 3D examples with known analytical solutions which are designed to demonstrate the theoretical predictions; while the last two are the well-known 2D lid-driven cavity flow and backward-facing step flow problems, which are used to investigate the convergence behaviour of the proposed method depending on the boundary data.

4.1 Analytical solution in 2D case

In this test case, the solution domain Ω is the unit square $[0,1]\times[0,1]$ in $\mathbb{R}^2$. The body force f and the boundary conditions are set such that the exact solution of the stationary Navier-Stokes equations is given by

$$
\begin{aligned}
&u_1=10x^2(x-1)^2y(y-1)(2y-1), &\text{(4.1a)}\\
&u_2=-10y^2(y-1)^2x(x-1)(2x-1), &\text{(4.1b)}\\
&p=3x^2+3y^2-2. &\text{(4.1c)}
\end{aligned}
$$

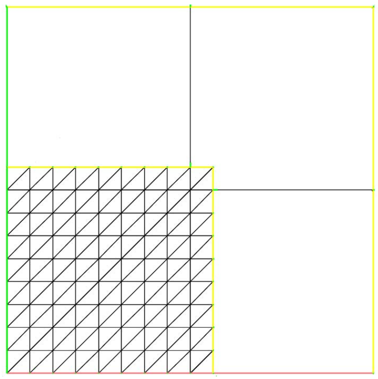

Figure 2: Triangulation and overlapping domain decomposition of Ω.

The numerical experiment is performed on a Dawning parallel cluster. Data exchanges between processors are supported by the Message Passing Interface (MPI). The mesh consists of triangular elements which are obtained by dividing Ω (or Ω_j, j=1,2,$\cdots$,J) into sub-squares of equal size and then drawing the diagonal in each sub-square; see Fig. 1. The Taylor-Hood mixed finite elements are employed for the discretization. To avoid the initial fan-out communication, we let all processors simultaneously compute the coarse solution in our numerical experiments.

Firstly, in order to test the asymptotical error provided by our parallel method, we set $\nu=0.1$ and divide $\Omega=[0,1]\times[0,1]$ into four disjoint subdomains:

$$D_1=(0,1/2)\times(0,1/2),\qquad D_2=(1/2,1)\times(0,1/2),$$
$$D_3=(0,1/2)\times(1/2,1),\qquad D_4=(1/2,1)\times(1/2,1),$$

and then extend each D_j $(j=1,2,3,4)$ outside with an extra layer of width h to obtain overlapped $\Omega_j\subset\Omega 4$ $(j=1,2,3,4)$; see Fig. 2.

We compute the finite element solutions by Algorithm 3.2 with fine meshes with size $h=n^{-3}$ $(n=3,4,5)$ and corresponding coarse meshes with size H satisfying $2H^3=h^2$. The corresponding linear algebraic systems are solved by LU factorization. The following stopping criterion (4.2) is employed for the nonlinear iteration on the coarse grid:

$$\frac{\|u_H^{n+1}-u_H^n\|_{0,\Omega}}{\|u_H^{n+1}\|_{0,\Omega}}<10^{-6}, \tag{4.2}$$

where u_H^n is the nth simple iterative solution. The numerical results are listed in Table 1 (top), in which m is the nonlinear iterations count satisfying the stopping condition (4.2). The convergence rates are computed by the formula $\frac{\log(E_i/E_{i+1})}{\log(h_i/h_{i+1})}$, where E_i and E_{i+1} are the relative errors

$$\frac{\||\nabla(u-u_m^h)|\|_{0,\Omega}+\||p-p_m^h|\|_{0,\Omega}}{\|\nabla u\|_{0,\Omega}+\|p\|_{0,\Omega}}$$

Table 1: Errors of the approximate solutions for 2D case.

Method	h	H	m	CPU(s)	$\frac{\|\|\|\nabla(u-u_m^h)\|\|\|_{0,\Omega}}{\|\|\nabla u\|\|_{0,\Omega}}$	$\frac{\|\|\|p-p_m^h\|\|\|_{0,\Omega}}{\|\|p\|\|_{0,\Omega}}$	rate
Algorithm 3.2	1/27	1/18	3	2.85	0.00380327	0.000355402	
	1/64	1/32	3	8.53	0.000726862	7.33137e-05	1.89088
	1/125	1/50	3	34.04	0.00020287	1.68941e-05	1.98901
Standard FE	1/27	-	3	5.02	0.00403434	0.000342939	
	1/64	-	3	47.37	0.000720131	6.1036e-05	1.99753
	1/125	-	3	816.41	0.000189005	1.60029e-05	1.99863

corresponding to the fine meshes with size h_i and h_{i+1}, respectively. While the CPU time in seconds is the wall time of the parallel program.

Let (u,p) be the exact solution to the Navier-Stokes equations and (u_m^h,p_m^h) be obtained by our parallel two-level finite element method. According to the mixed finite element spaces we chosen and the relationship between the mesh sizes H and h, i.e., $H=\mathcal{O}(h^{2/3})$, by Theorem 3.2, we have the following asymptotic behavior:

$$|||\nabla(u-u_m^h)|||_{0,\Omega}+|||p-p_m^h|||_{0,\Omega}\sim ch^2+C\|u_H^m-u_H^{m-1}\|_{0,\Omega}. \tag{4.3}$$

Moreover, if $C\|u_H^m-u_H^{m-1}\|_{0,\Omega}$ is a higher-order infinitesimal quantity compared to ch^2 as H (and hence h) tends to zero, we have the following asymptotic behavior:

$$|||\nabla(u-u_m^h)|||_{0,\Omega}+|||p-p_m^h|||_{0,\Omega}=\mathcal{O}(h^2).$$

The results shown in Table 1 (top) support the above estimate.

To compare with the standard Galerkin finite element method, in Table 1 (bottom), we also listed the errors of the global standard finite element solution computed by the simple iterative method, where m is the nonlinear iterations count satisfying the following stopping condition

$$\frac{\|u_h^{n+1}-u_h^n\|_{0,\Omega}}{\|u_h^{n+1}\|_{0,\Omega}}<10^{-6}. \tag{4.4}$$

From Table 1 we can see that our parallel finite element method is highly efficient. It can yield an approximate solution with an accuracy comparable to that of the global standard finite element solution with a large reduction in computational time.

In our numerical tests, we also computed the finite element solution with various values of the viscosity parameter ν. The numerical results show that when ν is smaller than 0.001, the algorithm doesn't work; this may be caused by that the stability condition (3.8) is not satisfied.

Secondly, to investigate how accurate should the coarse grid problem be solved, we set $\nu=0.01,0,005$, $h=1/125$, $H=1/50$ and then compute the finite element solution using Algorithm 3.2. At each simple nonlinear interation, we compute two quantities

$$\frac{|||\nabla(u-u_n^h)|||_{0,\Omega}}{\|\nabla u\|_{0,\Omega}} \quad \text{and} \quad \frac{|||\nabla(p-p_n^h)|||_{0,\Omega}}{\|p\|_{0,\Omega}},$$

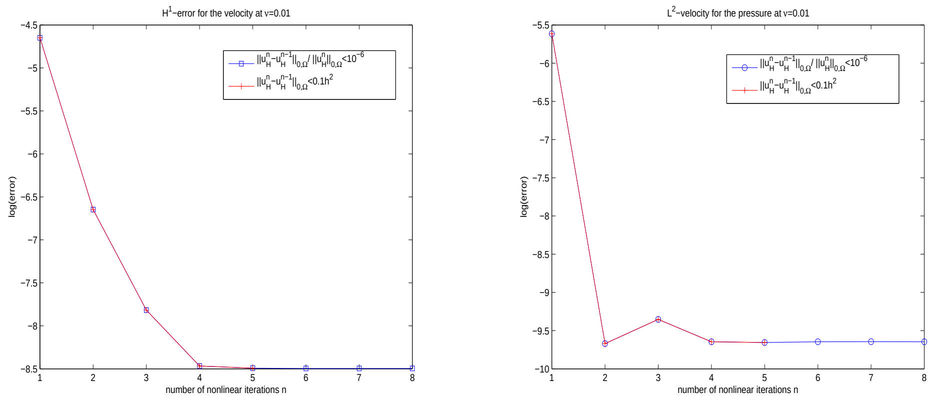

(a) (b)

Figure 3: Evolution of the errors with the number n of nonlinear iterations at $\nu=0.01$: $\||\nabla(u-u_n^h)|\|_{0,\Omega}/\|\nabla u\|_{0,\Omega}$ (a) and $\||p-p_n^h|\|_{0,\Omega}/\|p\|_{0,\Omega}$ (b).

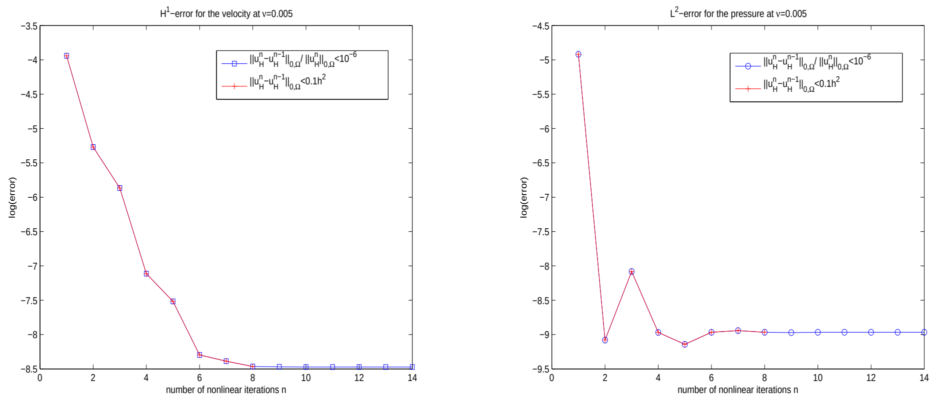

(a) (b)

Figure 4: Evolution of the errors with the number n of nonlinear iterations at $\nu=0.005$: $\||\nabla(u-u_n^h)|\|_{0,\Omega}/\|\nabla u\|_{0,\Omega}$ (a) and $\||p-p_n^h)|\|_{0,\Omega}/\|p\|_{0,\Omega}$ (b).

and investigate their evolution with the simple nonlinear iterations, where both the stopping conditions (4.2) and (3.22) with $c=0.1$ and $s=2$ are used.

Figs. 3 and 4 show that the stopping condition (3.22) is satisfied when the number of simple nonlinear iterations is 5 and 8 at $\nu=0.01$ and 0.005, respectively, while there are 8 and 14 steps nonlinear iterations when the stop condition (4.2) is satisfied. The numerical results indicate that it is enough for the coarse grid nonlinear problem to be solved with an accuracy that (3.22) is satisfied. Further iterations make no obvious contribution to the improvement in accuracy of the solution. From this test case, we can conclude that our derived stopping criterion (3.22) for the simple nonlinear iterations on the coarse grid is

Table 2: Wall time $T(J)$ in seconds of the parallel program, speedup $S_p=T(1)/T(J)$ and parallel efficiency $E_p=T(1)/J\times T(J)$.

J	1	2	4	6	8	12	16
$T(J)$	235.37	48.51	34.04	26.47	7.75	23.17	22.55
S_p	1.0	4.85	6.91	8.89	9.66	10.16	10.44
E_p	1.0	2.43	1.73	1.48	1.21	0.85	0.65

reliable and suitable, which can yield a good solution without redundant computations.

Finally, to check the parallel performance of our parallel finite element method, we decompose the solution domain into 1×2, 2×2, 2×3, 2×4, 3×4 and 4×4 subdomains of equal size, respectively, and then assign each processor a subdomain to compute the corresponding solution by Algorithm 3.2, where the mesh sizes are set as $h=1/125$, $H=1/50$. The overlapping size is $1/125\times 2$. Table 2 reports the wall time of the parallel program and the corresponding speedup and parallel efficiency computed by

$$S_p=\frac{T(1)}{T(J)}, \quad E_p=\frac{T(1)}{J\times T(J)}, \tag{4.5}$$

where $J>1$ is the number of processors (or subdomains), $T(1)$ and $T(J)$ are the wall time of the parallel program with one and J processors, respectively. From Table 2, we can see that our parallel algorithm has a good parallel performance. Especially, superlinear speedups and parallel efficiencies bigger than one were obtained when the number of processors is 2, 4, 6 and 8, respectively. This often observed effect for such "embarrassingly" parallel computations arises from the aggregate effect of the increasing amounts of cache memory available to store data for size-fixed problem.

It is remarked that from Table 2, one may see that as the number of processors increases from 8 to 12 and to 16, the parallel efficiency quickly drops. This is due to the redundant computations for the coarse grid problem which became a more significant fraction of the total computations for each processor (in our numerical experiments, the coarse grid problem was solved sequentially and independently by all processors, while the coarse grid size H was 1/50 leading to a big scale computation). Therefore, when the computational scale of the coarse grid problem is big, it is necessary to compute the coarse grid solution in parallel for a better parallel performance. This will be considered in our future work.

4.2 Analytical solution in 3D case

In this example, the exact solution to the Navier-Stokes equations is given by

$$\begin{aligned}
u_1&=x^2(x-1)^2[2y(y-1)(2y-1)z^2(z-1)^2-2y^2(y-1)^2z(z-1)(2z-1)],\\
u_2&=y^2(y-1)^2[-2x(x-1)(2x-1)z^2(z-1)^2+2x^2(x-1)^2z(z-1)(2z-1)],
\end{aligned}$$

$$u_3 = z^2(z-1)^2[2x(x-1)(2x-1)y^2(y-1)^2 - 2x^2(x-1)^2y(y-1)(2y-1)],$$
$$p = x^2+y^2+z^2-1,$$

where $\Omega=[0,1]\times[0,1]\times[0,1]$, which is decomposed into $2\times2\times2$ subdomains of equal size in our numerical test. The body force f is computed by (2.1a).

We first set $\nu=0.1$ and then compute the finite element solution with Algorithm 3.2 and another similar algorithm where the coarse grid nonlinear problem is solved by Newton iterations and the fine grid problem is the same as Algorithm 3.2 (we denote this algorithm as N-O Algorithm), where the stopping condition (3.22) with c=0.1 and $s=2$ is employed. The numerical results are listed in Table 3, which shows good agreement with the theoretical predictions. It is also shown that there is no difference between the computed solution by our Algorithm 3.2 and the N-O Algorithm; however, our proposed simplified iterative algorithm takes less computational time than the N-O Algorithm; the bigger the computational scale, the more the computational time saved by our proposed algorithm compared to the N-O algorithm.

Secondly, to further compare our simplified iterative algorithm with the N-O Algorithm, we set $h=1/8$, $H=1/4$ and then compute the finite element solution with various values of the viscosity ν. The numerical results listed in Table 4 show that as ν decreases to $\nu=10^{-6}$, both our algorithm and the N-O algorithm fail to work. This may be caused

Table 3: Errors of the computed solutions for 3D case.

Method	h	H	it	CPU(s)	$\|\|\|\nabla(u-u_m^h)\|\|\|_{0,\Omega}$	$\|\|\|p-p_m^h\|\|\|_{0,\Omega}$	rate
Algorithm 3.2	1/4	1/2	2	0.178997	0.0397858	0.0329596	-
	1/8	1/4	2	0.982288	0.00761281	0.00799658	2.22044
	1/12	1/6	2	4.24722	0.00283863	0.00355064	2.20303
	1/16	1/8	2	15.5743	0.00142742	0.00199967	2.16527
	1/20	1/10	2	48.4488	0.000868242	0.00128148	2.09001
N-O Algorithm	1/4	1/2	2	0.193378	0.0397858	0.0329596	-
	1/8	1/4	2	1.07044	0.00761281	0.00799658	2.22044
	1/12	1/6	2	4.5207	0.00283863	0.00355064	2.20303
	1/16	1/8	2	16.2599	0.00142742	0.00199967	2.16527
	1/20	1/10	2	49.6552	0.000868242	0.00128148	2.09001

Table 4: Comparison of the methods.

ν	Algorithm 3.2			N-O Algorithm		
	CPU(s)	$\|\|\|\nabla(u-u_m^h)\|\|\|_0$	$\|\|\|p-p_m^h)\|\|\|_0$	CPU(s)	$\|\|\|\nabla(u-u_m^h)\|\|\|_0$	$\|\|\|p-p_m^h)\|\|\|_0$
10^0	1.01357	0.000862893	0.00798686	1.09272	0.000862893	0.00798686
10^{-1}	0.982288	0.00761281	0.00799658	1.07044	0.00761281	0.00799658
10^{-2}	0.978332	0.0760202	0.00799817	1.0756	0.0760202	0.00799817
10^{-3}	0.992493	0.760167	0.0079984	1.06746	0.760167	0.0079984
10^{-4}	0.982308	7.57423	0.00800595	1.05945	7.57542	0.00800565
10^{-5}	0.979465	66.7898	0.00914237	2.17457	70.5172	0.00830664
10^{-6}	–	–	–	–	–	–

by the invalidation of the stability condition (3.8). For all values of ν being tested, there has no obvious difference between the computed solutions by the two methods; however, it is clearly shown that our proposed algorithm spends less computational time than the N-O Algorithm.

4.3 Lid-driven cavity flow

Here we consider the lid-driven cavity flow problem defined in the square domain $\Omega=[0,1]\times[0,1]$. With zero external body force, velocities are zero on all edges except the top one (the lid), which has a driving horizontal velocity of one.

We set $h=1/64$, $H=1/32$ and compute the finite element solution by our Algorithm 3.2, where the stopping condition (3.22) for nonlinear iterations on the coarse grid is employed. Figs. 5 and 6 show the computed streamlines and isobars at $\nu=1$ and 0.1, respectively, with four subdomains. This test case illustrated the effectiveness of the pro-

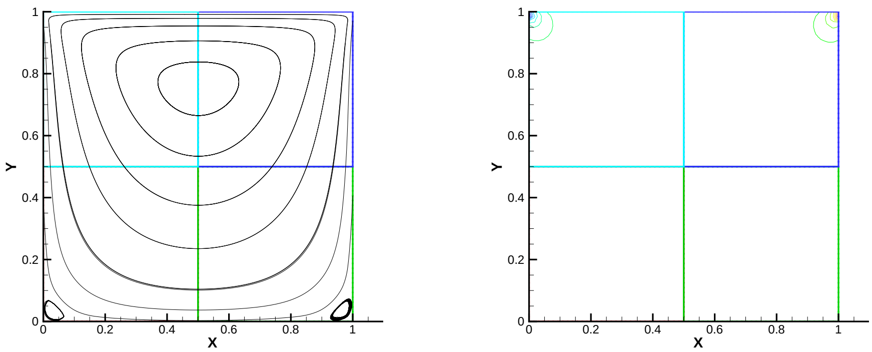

(a) (b)

Figure 5: Computed streamlines (a) and isobars (b) for the lid-driven cavity flow at $\nu=1$.

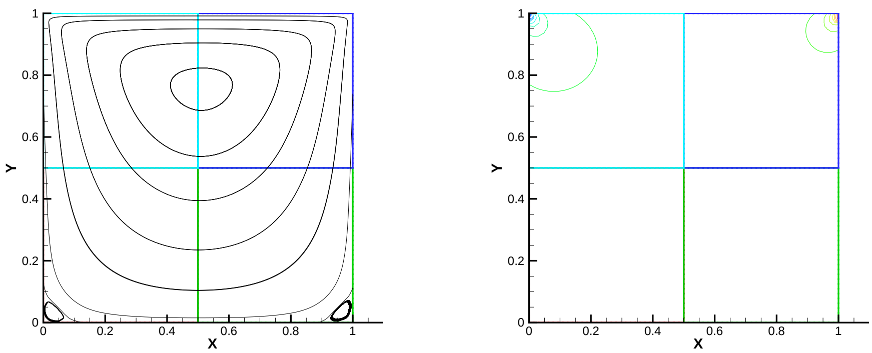

(a) (b)

Figure 6: Computed streamlines (a) and isobars (b) for the lid-driven cavity flow at $\nu=0.1$.

posed algorithm.

4.4 Backward-facing step flow

In this example, we consider the 2D backward-facing step flow which is a significant test problem for validating the robustness of a Navier-Stokes solver. This problem is defined on a long channel $[0,30]\times[-0.5,0.5]$, with no-slip conditions imposed on the top and bottom walls, as well as the lower half of the left boundary. At the inlet boundary, a fully developed parabolic velocity profile $u_1=24y(0.5-y)$ for $0\le y\le 0.5$ is specified. See Fig. 7 for detailed geometry and boundary conditions information.

We decompose the flow domain into 5×1 disjoint sub-domains of equal size, and then extend each sub-domain outside with an extra layer of size h. The quasi-uniform meshes sizes are set as $H=1/32$, $h=1/64$. Figs. 8 and 9 depict the computed streamlines and isobars, which illustrated the effectiveness of our proposed method.

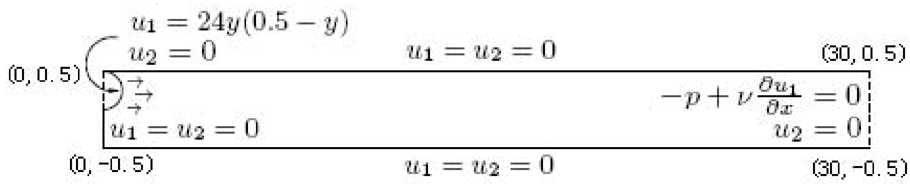

Figure 7: Schematic diagram of the backward-facing step flow.

(a) (b)

Figure 8: Computed streamlines for backward-facing step flow at $\nu=1$ (a) and $\nu=0.1$ (b).

(a) (b)

Figure 9: Computed isobars for backward-facing step flow at $\nu=1$ (a) and $\nu=0.1$ (b).

5 Conclusions

In this work, we have presented and analyzed a simplified parallel two-level iterative finite element method for the incompressible Navier-Stokes equations. It is based on a coarse grid nonlinear problem which is solved by a simple iterative method and local fine grid linearized Oseen correction problems defined in overlapped subdomains. Under some appropriate regularity assumptions and the stability condition, error bounds of the approximate solution were estimated. Numerical tests have also been performed which illustrated the effectiveness of the proposed method.

Acknowledgments

This work was supported by the Natural Science Foundation of China (No. 11361016), the Project Sponsored by the Scientific Research Foundation for the Returned Overseas Chinese Scholars, State Education Ministry, the Scientific Research Foundation of Southwest University, Fundamental Research Funds for the Central Universities (No. XDJK2014C160, SWU113095), and the Science and Technology Foundation of Guizhou Province, China (No. [2013]2212).

We appreciate the valuable comments and suggestions given by the reviewers, which lead to a large improvement of the paper.

References

[1] J. C. Xu and A. H. Zhou, *Local and parallel finite element algorithms based on two-grid discretizations,* Math. Comput., 69 (2000), pp. 881–909.

[2] J. C. Xu and A. H. Zhou, *Local and parallel finite element algorithms based on two-grid discretizations for nonlinear problems,* Adv. Comput. Math., 14 (2001), pp. 293–327.

[3] Y. N. He, J. C. Xu and A. H. Zhou, *Local and parallel finite element algorithms for the Navier-Stokes problem,* J. Comput. Math., 24(3) (2006), pp. 227–238.

[4] Y. C. Ma, Z. M. Zhang and C. F. Ren, *Local and parallel finite element algorithms based on two-grid discretization for the stream function form of Navier-Stokes equations,* Appl. Math. Comput., 175 (2006), pp. 786–813.

[5] F. Y. Ma, Y. C. Ma and W. F. Wo, *Local and parallel finite element algorithms based on two-grid discretization for steady Navier-Stokes equations,* Appl. Math. Mech., 28(1) (2007), pp. 27–35.

[6] Y. Q. Shang, *A parallel two-level linearization method for incompressible flow problems,* Appl. Math. Lett., 24 (2011), pp. 364–369.

[7] Y. Q. Shang, Y. N. He, D. W. Kim and X. J. Zhou, *A new parallel finite element algorithm for the stationary Navier-Stokes equations,* Finite Elem. Anal. Des., 47 (2011), pp. 1262–1279.

[8] Y. Q. Shang, Y. N. He and Z. D. Luo, *A comparison of three kinds of local and parallel finite element algorithms based on two-grid discretizations for the stationary Navier-Stokes equations,* Comput. Fluids, 40 (2011), pp. 249–257.

[9] Y. N. He, L. Q. Mei, Y. Q. Shang and J. Cui, *Newton iterative parallel finite element algorithm for the steady Navier-Stokes equations,* J. Sci. Comput., 44(1) (2010), pp. 92–106.

[10] Y. Q. Shang and Y. N. He, *A parallel Oseen-linearized algorithm for the stationary Navier-Stokes equations,* Comput. Methods Appl. Mech. Eng., 209-212 (2012), pp. 172–183.

[11] Y. Q. Shang, *A parallel two-level finite element variational multiscale method for the Navier-Stokes equations,* Nonlinear Anal., 84 (2013), pp. 103–116.

[12] Y. Q. SHANG AND S. M. HUANG, *A parallel subgrid stabilized finite element method based on two-grid discretization for simulation of 2D/3D steady incompressible flows,* J. Sci. Comput., 60 (2014), pp. 564–583.

[13] R. ADAMS, Sobolev Spaces, Academic Press Inc., New York, 1975.

[14] J. G. HEYWOOD AND R. RANNACHER, *Finite element approximation of the nonstationary Navier-Stokes problem I: Regularity of solutions and second-order error estimates for spatial discretization,* SIAM J. Numer. Anal., 19(2) (1982), pp. 275–311.

[15] V. GIRAULT AND P. A. RAVIART, Finite Element Methods for Navier-Stokes Equations: Theory and Algorithms, Springer-Verlag, Berlin, Heidelberg, 1986.

[16] R. TEMAM, Navier-Stokes Equations, North-Holland, Amsterdam, 1984.

[17] Y. Q, SHANG AND Y. N. HE, *Parallel iterative finite element algorithms based on full domain partition for the stationary Navier-Stokes equations,* Appl. Numer. Math., 60(7) (2010), pp. 719–737.

[18] Y. Q. SHANG AND K. WANG, *Local and parallel finite element algorithms based on two-grid discretizations for the transient Stokes equations,* Numer. Algor., 54 (2010), pp. 195–218.

[19] D. N. ARNOLD AND X. LIU, *Local error estimates for finite element discretizations of the Stokes equations,* RAIRO M^{2}AN, 29 (1995), pp. 367–389.

[20] D. N. ARNOLD, F. BREZZI AND M. FORTIN, *A stable finite element for the Stokes equations,* Calc., 21 (1984), pp. 337–344.

[21] M. FORTIN, Calcul Numérique des Ecoulements Fluides de Bingham et des Fluides Newtoniens Incompressible par des Méthodes D'eléments Finis, Doctoral thesis, Université de Paris VI, 1972.

[22] P. HOOD AND C. TAYLOR, *A numerical solution of the Navier-Stokes equations using the finite element technique,* Comput. Fluids, 1 (1973), pp. 73–100.

[23] M. CROUZEIX AND P. A. RAVIART, *Conforming and nonconforming finite element methods for solving the stationary Stokes equations,* RAIRO Anal. Numér., 7(R-3) (1973), pp. 33–76.

[24] L. MANSFIELD, *Finite element subspaces with optimal rates of convergence for stationary Stokes problem,* RAIRO Anal. Numér., 16 (1982), pp. 49–66.

[25] O. A. LADYZHENSKAYA, The Mathematical Theory of Viscous Incompressible Flows, Gordon and Breach, New York, 1969.

[26] Y. N. HE AND J. LI, *Convergence of three iterative methods based on finite element discretization for the stationary Navier-Stokes equations*, Comput. Methods Appl. Mech. Eng., 198 (2009), pp. 1351–1359.

[27] H. XU AND Y. N. HE, *Some iterative finite element methods for steady Navier-Stokes equations with different viscosities*, J. Comput. Phys., 232 (2013), pp. 136–152.